ORIGINAL PAPER

RJME
Romanian Journal of Morphology & Embryology
http://www.rjme.ro/

In vivo confocal microscopy quantification of reactive oxygen species: a working model in rat kidney

ADRIAN OVIDIU VĂDUVA[1)], COSMIN GLĂMEANU[2)], ROMEO NEGREA[3)], MIRELA DANINA MUNTEAN[4,5)], ALIS LILIANA CARMEN DEMA[1)]

[1)]*Department of Morphopathology, "Victor Babeş" University of Medicine and Pharmacy, Timişoara, Romania*

[2)]*"Pius Brânzeu" Center for Flap Surgery and Microsurgery, Timişoara, Romania*

[3)]*Department of Mathematics, Politehnica University of Timişoara, Romania*

[4)]*Department of Pathophysiology, "Victor Babeş" University of Medicine and Pharmacy, Timişoara, Romania*

[5)]*Center for Translational Research and Systems Medicine, "Victor Babeş" University of Medicine and Pharmacy, Timişoara, Romania*

Abstract

Oxidative stress is a culprit responsible for the development of acute and chronic kidney diseases. We aimed to establish a working model for the dynamic *in vivo* assessment of reactive oxygen species (ROS) production in rat kidney. A randomized controlled study was performed in 36 adult male Wistar rats subjected to unilateral urinary obstruction (UUO) *via* ureteral ligation and compared to SHAM controls. Dihydroethidium (DHE) was injected in the femoral vein and *in vivo* confocal microscopy was performed in the 2nd, 6th and 10th day, respectively after surgery. Maximal ROS levels elicited by UUO were recorded on the 6th day. However, the absolute difference of the means of DHE fluorescence intensity between UUO and SHAM was the highest on the 10th day. Our working model can monitor ROS production at different time frames and our initial findings suggest that the surgery-related ROS levels decline after an initial increase in the first days, whereas the ones elicited by chronic ligation continue to raise.

***Keywords*:** ureteral ligation, rat, oxidative stress, *in vivo* confocal microscopy, Dihydroethidium.

Introduction

Reactive oxygen species (ROS) are highly reactive chemical intermediates generated during oxygen metabolism. Superoxide anion constitutes the primarily oxyradical produced mainly during the activity of the mitochondrial electron transport chain that can be further converted into other ROS, namely hydrogen peroxide and the hydroxyl radical. Moreover, superoxide can react with nitric oxide with the subsequent formation of peroxynitrite, a damaging reactive nitrogen species [1]. The deleterious effects of the reactive oxygen and nitrogen species consist in the widespread damage of several macromolecules, including nucleic acids, lipids and proteins [2]. The imbalance between the increased ROS production and/or the decreased antioxidant defense of the cells defines the oxidative stress (OS) [3]. In the setting of renal OS, the cell signaling mechanisms are disturbed which, in turn, trigger the loss of cellular structures through apoptosis and the promotion of tissue fibrosis, eliciting the progression towards chronic kidney disease (CKD) [4]. Experimental studies demonstrated that in transplanted kidneys with chronic allograft nephropathy, OS was increased in all structures of the renal parenchyma [5]. In kidney allografts, Djamali described the association between high OS in the presence of interstitial fibrosis and tubular atrophy; however, this author did not demonstrate a causal relation between the high levels of ROS and progression towards graft loss [6]. Evidence of increased OS was also present in the serum of patients in the early stages of CKD prior to the introduction of hemodialysis therapy [7].

Direct identification of cellular ROS in tissue samples is currently performed using fluorescent probes. Quantification of ROS generation can be achieved on various samples, such as frozen tissue samples, kidney slice models, *ex vivo* isolated perfused kidney, *in vivo* labeling followed by the analysis of the frozen tissue, as well as direct *in vivo* kidney imaging [8–13].

Since ROS lifetime is short and OS levels may be artificially altered by the *ex vivo* processing of tissues on ice, the *in vivo* assessment of oxidative stress represents the most reliable method that allows the appropriate ROS quantification.

Dihydroethidium (DHE) is a cell permeable fluorescent marker with DNA affinity commonly used for the quantification of superoxide anion [14]. In the presence of superoxide, DHE generates two major fluorescent products: Ethidium and 2-Hydroxyethidium, the former being generated by several oxidants, while the latter resulting only through oxidation by superoxide [15]. The fluorescence spectrum of DHE shows two excitation peaks. It has been documented that excitation at 396 nm elicits a more specific response from superoxide generated 2-Hydroxyethidium than at 510 nm, where there is an overlap in emission spectra from the non-superoxide generated Ethidium [16].

It is widely accepted that mitochondria are the major site for ROS production in all mammalian cells [1]. Our experience with laser scanning *in vivo* imaging showed that we could not reach sufficient resolution to isolate

mitochondrial-derived signals; thus, for the proper *in vivo* quantification of ROS we assessed the cytoplasmic signal. However, acute kidney injury leads to mitochondrial conformational changes represented mostly by fission, fragmentation and outer membrane permeabilization [17], which will lead to the ROS leakage in the cytoplasm, thus increasing the intensity of nuclear DNA-bound DHE signal.

Quantification of the DHE nuclear staining is often performed by analyzing the fluorescence emission intensity [18]. Less frequently encountered is the technique of counting the positively stained nuclei in a population of cells labeled with 4',6-Diamidino-2-phenylindole (DAPI) [19].

The aim of the present study was to establish a working model for the evaluation of the *in vivo* ROS production after a single intravenous DHE injection in experimentally induced unilateral urinary obstruction (UUO) in rats at different timeframes, using confocal microscopy imaging.

Materials and Methods

We performed a randomized control study on adult male Wistar rats to assess kidney DHE fluorescence intensity *in vivo* using confocal microscopy imaging.

Rats were purchased from the "Cantacuzino" Institute (Bucharest, Romania) and allowed to acclimate for two weeks in the Animal Housing Unit of our University, under controlled environmental conditions: constant temperature (22 ± 2^0C) and humidity, in 12 hours light and dark cycles. Unrestricted access to water and food was provided throughout the entire duration of the experiments. Food restriction was applied only on the day preceding the microscopic *in vivo* examination, in order to have the large bowel void of feces, thus allowing an easier access to the kidney *via* abdominal incision.

The experimental procedures were performed following the 2010/63/EU Directive and Romanian Law No. 43/2014 regarding protection of the animals used in scientific experiments. Approval from the Research Ethics Committee of the "Victor Babeş" University of Medicine and Pharmacy, Timişoara, Romania was obtained (No. 04/20.03.2014).

Induction of unilateral urinary obstruction

Adult male Wistar rats were randomized into six groups: three groups were subjected to left ureteral ligation in order to produce UUO and three groups were sham-operated (Figure 1).

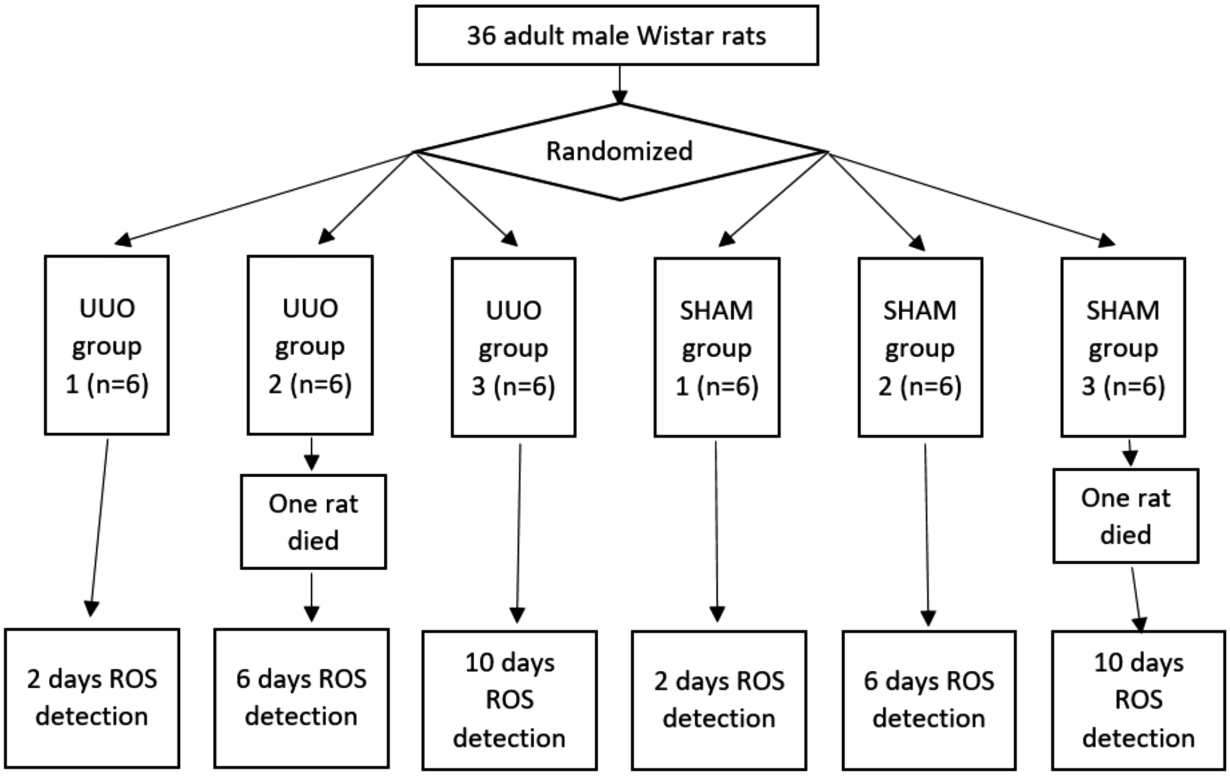

Figure 1 – ***Schematic illustration of the experimental protocol. UUO: Unilateral urinary obstruction; ROS: Reactive oxygen species.***

Evaluation of the right kidney in the same ligated rats could have been influenced by the compensatory changes occurring in the non-operated one; therefore, we did not use that one as control. Instead, we chose to use sham-operated rats as controls in order to recapitulate the surgical stress on the same kidney.

Initial surgical procedures were performed at the "Pius Brânzeu" Centre for Flap Surgery and Microsurgery, Timişoara, Romania, under inhalatory anesthesia with Isoflurane, using a Leica-Wild M650 surgical microscope. UUO was induced according to a previously described technique [20]. Briefly, the left ureter was exposed *via* abdominal incision and ligated with an 8.0 suture (ETHICON). The ceasing of the ureteral peristaltic movements was visually documented in every ligated rat.

Sham-operated rats had their left ureter exposed, without performing ligation, followed by closure of the abdominal incision. The rats were then allowed to recover until the day of microscopic examination.

In vivo confocal microscopy examination

All animals were subjected to examination in confocal microscopy, at 2, 6 and 10 days after surgery. Deep anesthesia was induced *via* intramuscular injection of a cocktail (0.1 mL/100 g body weight) of Ketamine (0.6 mL/ 1 mL cocktail, 10% Ketamine), Xylazine (0.3 mL/1 mL cocktail, Xylazin BIO 2%) and Acepromazine (0.1 mL/ 1 mL cocktail, Acepromazine maleate 20 mg/mL).

The initial abdominal wound was reopened and the left kidney was exposed by gentle blunt dissection. Positive control for UUO was left ureter dilation detected by visual inspection with the corresponding kidney looking enlarged and hyperemic. No signs of fistulization were identified. The fluorescence labeling for ROS generation was performed by injecting 1 mg/kg DHE (Sigma-Aldrich, D7008) in the femoral vein.

In vivo imaging was performed as previously described [21] on a laser scanning confocal microscope (Olympus Fluoview FV1000) using a 20× NA=0.75 Plan Super Apochromat objective. Image acquisition was done using 405 nm and consecutively, 488 nm excitation, while emission was detected using a barrier filter (BF) positioned at 555 nm, BF range 100 nm. We used a custom-built metal plate with a round hole in the middle and on top of that, we taped a coverslip. The rat was set flat on its abdomen, the kidney lying on the coverslip. We used no other means of securing the kidney to the coverslip, except the own bodyweight of the rat. Core temperature was maintained at 37–38^{0}C with the aid of a heated textile blanket.

For each rat, representative time-lapse image stacks (50 images/stack, one-second interval) were recorded to compensate for respiration and pulse-induced artifacts.

At the end of the experiment, the rats were euthanized and the left kidneys were harvested and fixed in formalin for paraffin embedding. The resulting histological slides were stained using Hematoxylin–Eosin (HE) and Periodic Acid–Schiff (PAS) techniques.

Image analysis

We performed automated and semi-automated image analysis using the Icy open source bioimage analysis software ver. 1.6.1.1. [22]. DHE fluorescence intensity was measured as integrated fluorescence intensity (IFI), taking into account both cytoplasmic and nuclear signals. An automated processing protocol was constructed to measure all pixel intensities in each acquired image and compute the IFI as the sum of all these.

Separately, from each 50-image time-lapse stack at least three images were selected, avoiding as much as possible the use of pictures that presented motion artifacts. Nuclei were visually identified based on their morphology, included into larger regions of interest, which were then restrained to proper the nuclear contour using the Active Cells plugin [23]. For each segmented nucleus, we determined the average fluorescence intensity (Figure 2, a and b).

Statistical analysis

We separated the previously acquired values into four analysis groups (AG), to characterize the time-dependency factor: sham – 405 nm laser excitation (S405), sham – 488 nm excitation (S488), ligated – 405 nm excitation (L405) and ligated – 488 nm excitation (L488).

All data were expressed as means ± standard error of the mean (SEM). We performed Student's *t*-test, Analysis of Variance (ANOVA) test and Tukey's multiple comparison test for significance [24]. A *log-log* generalized linear model [25] was proposed to test if there is an identifiable relationship between the results obtained at different time points. A $p<0.05$ value was considered statistically significant.

Results

Experimental protocol and data set acquisition

Thirty-six Wistar rats (n=6/group) were randomly assigned to six experimental groups (EG): three groups undergoing UUO and three groups SHAM operated, respectively (Figure 1). As two rats died prior to *in vivo* imaging (from the ligated 6th day group and SHAM 10th day group, respectively), confocal microscopic examination was performed on 34 rats.

The above-described setup allowed us to visualize up to an average depth of 60 μm into the kidney cortex, identifying renal tubules. The surface of the kidney available for examination was limited by two major factors: the convex shape of it and the adjacent organs, which were not surgically removed to give a broader viewing window. For each rat, we acquired time-lapse stacks (50 images) from at least three randomly selected microscopic fields, covering all identified DHE positively stained nuclei. From every stack, we selected at least three representative images to analyze nuclear staining. For identical nuclei within the image sets, an average value of the fluorescence intensity was calculated.

IFI quantification

In all rat groups, we identified higher ROS levels on the 6th day as compared to the 2nd and 10th day. The ANOVA analysis performed for four AG showed significant p values (S405 – p=0.0106; L405 – p=0.033; S488 – $p<0.0001$; L488 – p=0.0298). When we compared the average values for each EG, we noticed overall higher values for ligated *vs.* sham in 405 nm excitation assays and higher values for sham group in 488 nm assay (Figure 3, a and b). In the 405 nm assay, we identified significant differences between the 2nd and 6th days in both sham (p=0.0013) and ligated groups (p=0.0128). In the 488 nm excitation dataset, we identified significant differences between the 2nd and 6th day in both sham ($p<0.0001$) and ligated (p=0.017) groups, between 6th and 10th day in sham (p=0.005) and between sham and ligated on the 6th day (p=0.0071).

To assess the sole contribution of the ligation to the ROS levels, we analyzed the absolute difference of the means of UUO and SHAM and noticed that on the 6th day the levels were lower than on the 2nd day, which was more pronounced for the 488 nm excitation, but later rose on the 10th day. In the 405 nm excitation assay, the values were higher on the 10th day in comparison to the 2nd day (Figure 3c).

Nuclear DHE levels in ligated rats

The maximum levels of nuclear DHE labeling were identified on the 6th day after ligation (Figure 2d). On the 10th day, the levels were lower than on the 6th day (Figure 2e). ANOVA analysis showed very significant differences (p<0.0001), while Tukey's multiple comparison test showed significant differences between the 2nd and 6th, respectively 6th and 10th, for both 405 nm and 488 nm excitation assays.

Nuclear DHE labeling levels in sham-operated rats

We detected an increase in levels of the ROS generation from the second day, with maximum staining intensity in all detections being identified on the 6th day after intervention. Interestingly, on the 10th day the levels were lower when compared to the ones recorded in the 6th day, for both 405 nm and 488 nm excitation settings (Figure 4, a and b). ANOVA analysis showed very significant differences (p<0.0001), while Tukey's multiple comparison test showed significant differences between the 2nd and 6th, respectively 2nd and 10th, for both 405 nm and 488 nm excitation assays.

Nuclear UUO *vs.* SHAM intensity

We identified similar trends in ROS production levels throughout the three timeframes. The timeframe comparison between SHAM and UUO showed significant difference in signal intensity only on the 10th day in both 405 nm (p=0.0052) and 488 nm (p=0.0021) (Figure 4) excitation assays, when ROS levels were higher in ligated rats.

We analyzed the absolute difference of the means of UUO and SHAM at 405 nm emission (Figure 4c), which revealed higher ROS generation on the 2nd and 6th days, with no significant differences between these two timeframes. On the 10th day, the absolute difference between UUO and SHAM showed a marked increase in DHE fluorescence intensity. The 488 nm comparison of the same parameters yielded a negative value on the 6th day (Figure 4d).

Number of nuclei

The average number of positive nuclei was higher for UUO *vs.* SHAM in both emission settings for the 2nd and 6th day, without reaching statistical significance. We identified a categorical generalized linear relationship for both SHAM groups (405 nm and 488 nm excitation) at 10 days in respect to six and two days (p-value <1%). This relationship was not valid for UUO groups (p-value >60%). There is a good relationship between UUO and SHAM at 405 nm excitation only on the 6th day (p-value <10%). We identified strong relationships between UUO and SHAM groups at 488 nm excitation on both 6th and 10th day after ligation (p-value <1%).

Histological analysis of harvested tissue

We examined the formalin-fixed, paraffin-embedded tissue specimens in optical microscopy and noticed that the tubular lumens gradually dilate from the 2nd to the 10th day. In the affected tubules, the epithelial cells were flattened. We noticed no remarkable inflammatory infiltrates or interstitial expansion due to fibrosis. The glomeruli appeared to be within normal histological limits (Figure 5).

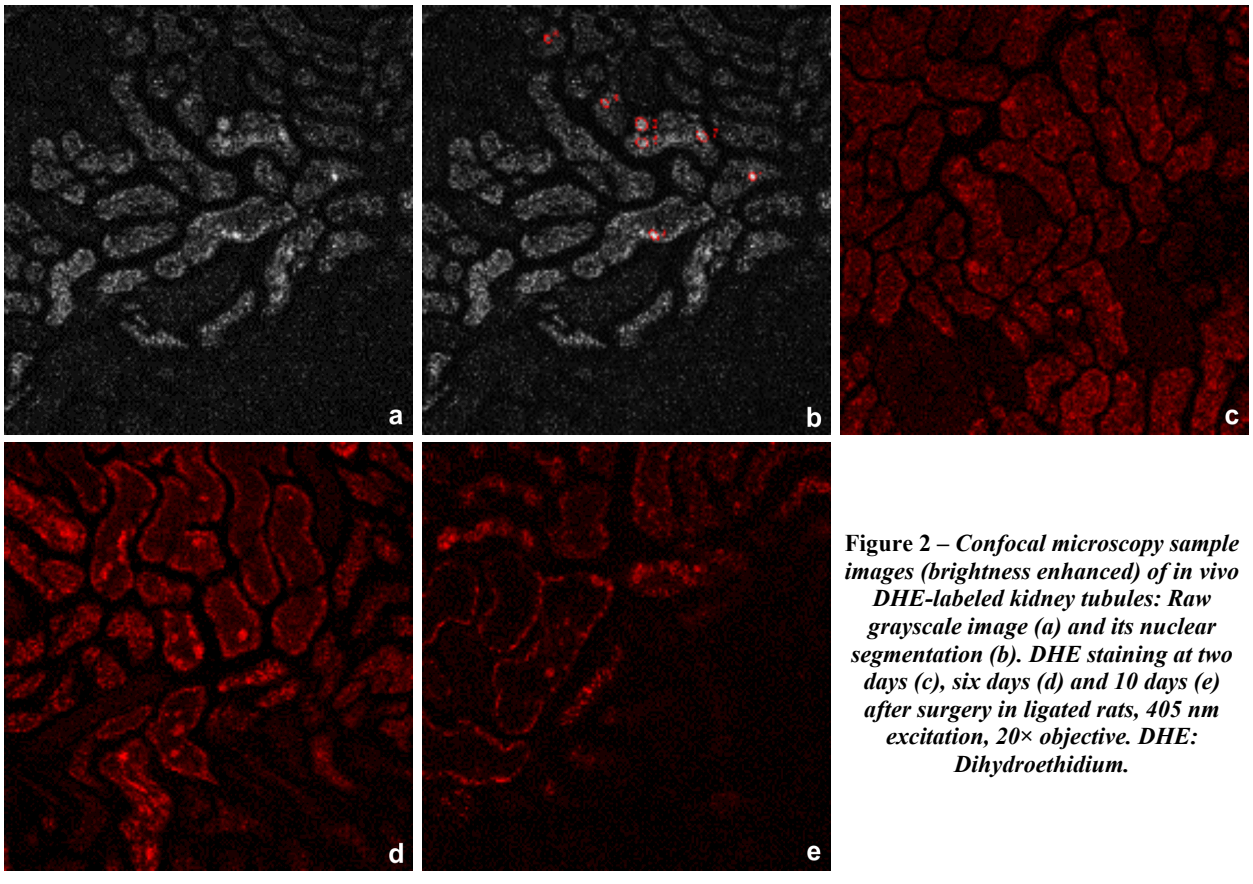

Figure 2 – ***Confocal microscopy sample images (brightness enhanced) of in vivo DHE-labeled kidney tubules: Raw grayscale image (a) and its nuclear segmentation (b). DHE staining at two days (c), six days (d) and 10 days (e) after surgery in ligated rats, 405 nm excitation, 20× objective. DHE: Dihydroethidium.***

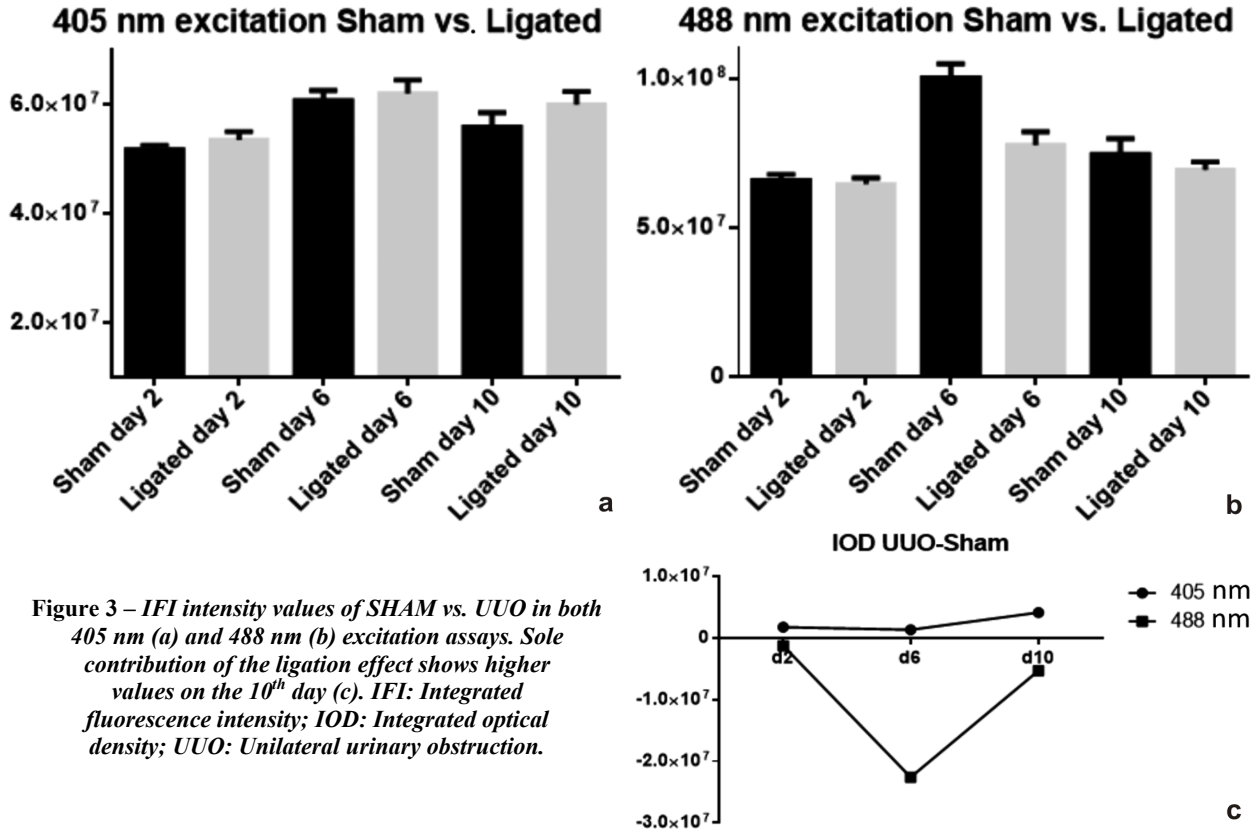

Figure 3 – ***IFI intensity values of SHAM vs. UUO in both 405 nm (a) and 488 nm (b) excitation assays. Sole contribution of the ligation effect shows higher values on the 10th day (c). IFI: Integrated fluorescence intensity; IOD: Integrated optical density; UUO: Unilateral urinary obstruction.***

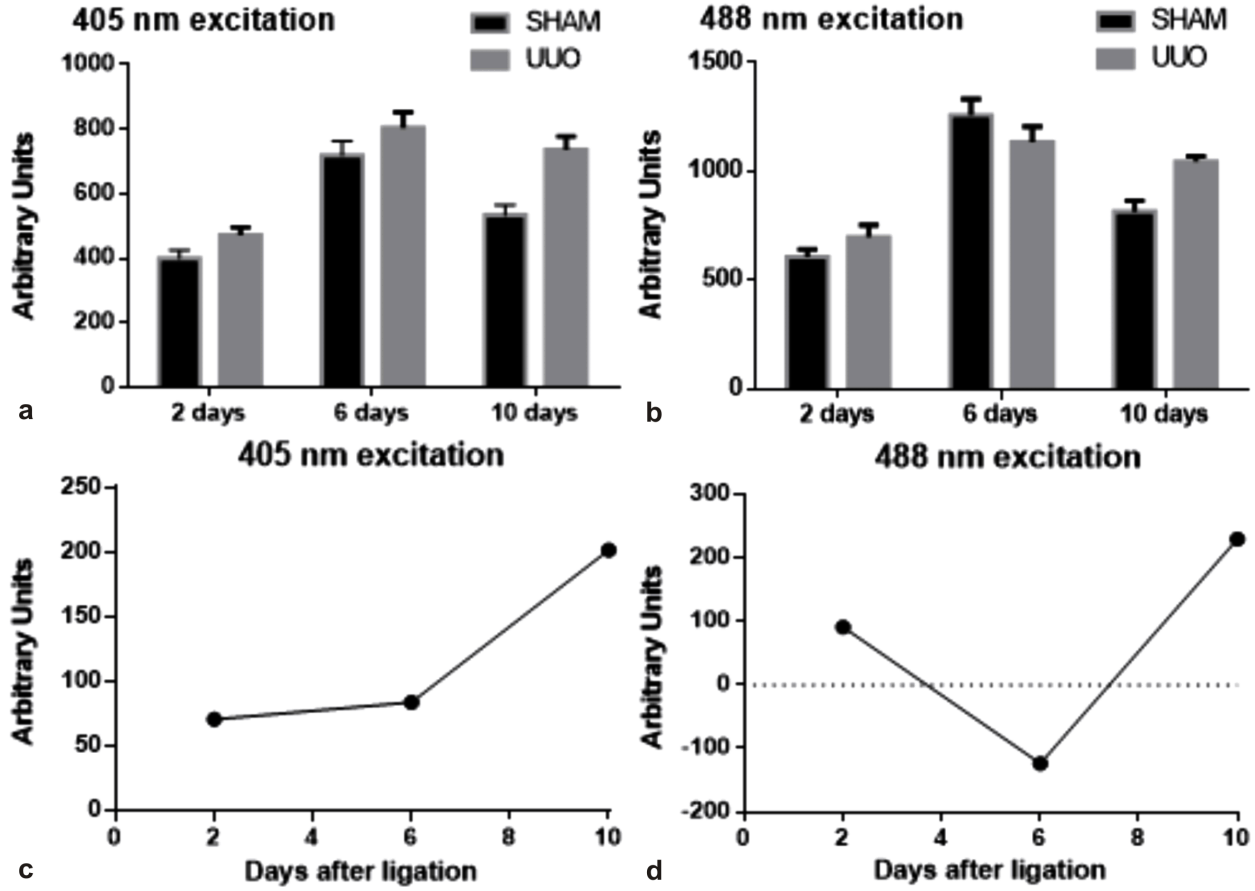

Figure 4 – ***Nuclear fluorescence intensity in SHAM vs. UUO at 405 nm (a) and 488 nm (b) excitation shows higher ROS levels in both assays on the 10th day for ligated rats. The ligation effect, as calculated by subtracting the mean values of SHAM from UUO, shows an increasing trend for the 405 nm excitation assay (c), while in 488 nm stimulus setting (d) it shows a marked increase from the 6th to the 10th day. UUO: Unilateral urinary obstruction; ROS: Reactive oxygen species.***

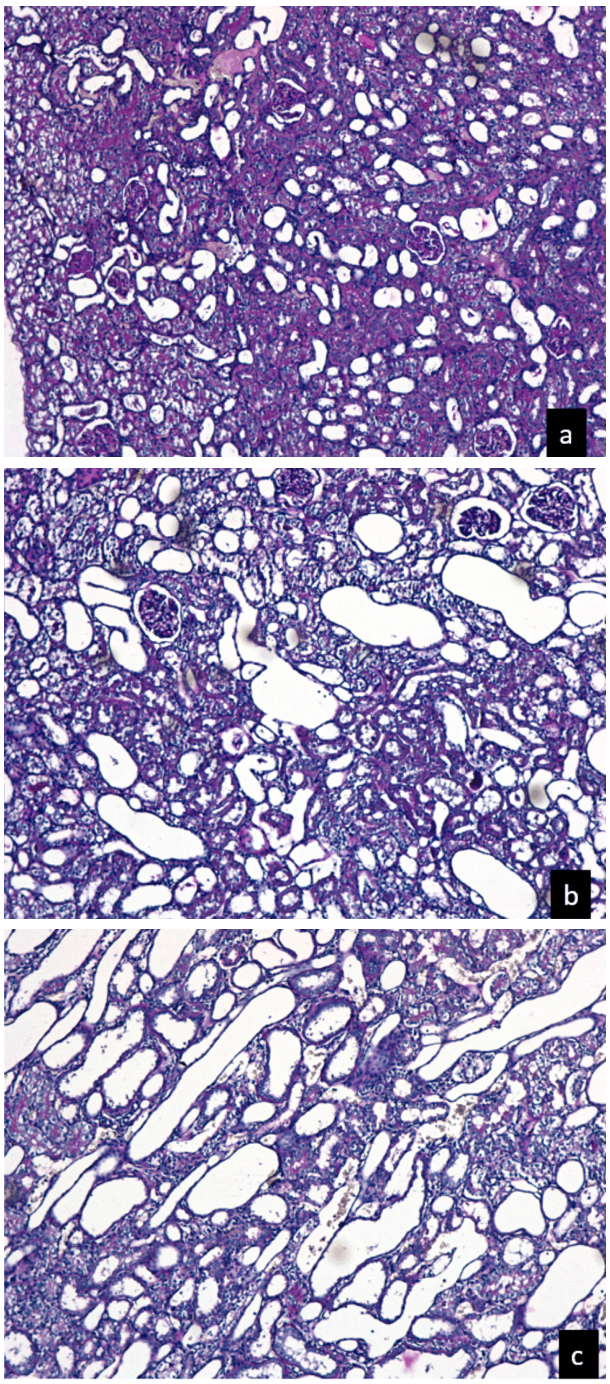

Figure 5 – ***Representative PAS-stained sections (×100) showing gradual dilatation of tubular lumens starting from the 2nd day (a), more prominent on the 6th day (b), reaching maximum on the 10th day (c). PAS: Periodic Acid–Schiff.***

Discussion

The present study aimed to establish a working experimental model for assessing the dynamics of ROS generation in the early stages of UUO-induced chronic damage in rat kidney using DHE as a marker to be quantified by *in vivo* confocal microscopy, followed by image analysis.

As previously mentioned, ROS generation occurs mostly in mitochondria. It has been shown that in the setting of acute kidney injury, mitochondrial activity is dysregulated, which leads to decreased cell respiration [26]. This observation may explain the low levels of ROS that were detected in ligated rats, in comparison to sham, when using the 488 nm excitation.

Furthermore, acute kidney injury leads to mitochondrial changes in conformation, represented mostly by fission, fragmentation and outer membrane permeabilization [17] leading to increased ROS production [27], which explains why the DHE fluorescent signal becomes detectable also at nuclear level, not just in the cytoplasm. It is tempting to speculate that a higher number of positively stained nuclei correlates to more widespread mitochondrial damage, hence increased ROS leaking into the cytoplasm, which will in turn trigger cellular injury and apoptosis, paving the way to nephron loss and subsequent fibrosis.

One major finding of this paper is that we detected significant increase in superoxide generated 2-Hydroxy-ethidium levels in UUO animals as compared to the sham-operated ones on the 10th day post-ligation. Of note, despite the fact that differences among the operated animals and their corresponding shams were also evident in the 2nd and 6th days, respectively, no statistical significance was found. This finding suggests that the surgery-related oxidative stress declines in the first days, whereas the one elicited by the chronic ligation continues to increase. In order to examine the contribution to ROS generation from ligation alone, we performed the subtraction of the absolute means of fluorescence intensity of SHAM from UUO values. Interestingly, using the 405 nm excitation, there was little difference between the values from the 2nd to the 6th days post-ligation. On the 10th day, we noticed a more than two fold increase in fluorescence intensity, noted on both IFI and nuclear quantification assays.

It has been reported in the literature that morphological changes (tubular atrophy, interstitial fibrosis) are present on histological analysis as early as 5–7 days after unilateral ureter ligation [28]. We were not able to recapitulate these observations on the histological evaluation of the samples. In our hands, only reversible histological changes throughout the entire timeline (tubular dilation with flattening of the epithelial cells) could be detected, while features of established chronic kidney injury (tubular atrophy, interstitial fibrosis) were absent.

An *in vivo* study on glomerular neutrophil infiltration using two-photon microscopy showed that inflammatory cells are crucial in triggering dysfunction in this renal compartment [29]. Linking our observations with the above-mentioned morphological findings, it appears that OS increases dramatically once the morphological changes become evident.

Several reports in the literature already acknowledged the caveats of using DHE for superoxide quantification, due to its two main oxidation products, Ethidium and 2-Hydroethidium [2, 15], since Ethidium can arise from non-superoxide oxidation of DHE [30]. Examining our 488 nm excitation results, we found lower levels of ROS in UUO rats compared to the SHAM-operated animals in IFI quantification. In line with this observation, we might assume that either other ROS (not superoxide) contribute to the elevated DHE values in SHAM rats or the superoxide anion is generated in a lesser extent in

the UUO rats. However, for the 10th day, both in 405 nm and 488 nm excitation assays, the nuclear fluorescence intensity was significantly higher in UUO *vs*. SHAM.

This finding is in line with the observation that 488 nm excitation is less specific to superoxide levels. It is tempting to speculate that in SHAM group the alternate routes for the generation of Ethidium are more prominent than in UUO. In our hands, the images generated at 405 nm excitation had less cytoplasmic background than the 488 nm ones, which made the nuclear identification easier.

We also noticed that there was no significant difference in the number of nuclei between the groups or the time-frames. However, we managed to identify a generalized linear relationship for a dynamic and predictive analysis by employing a *log-log* model (*i.e.*, the average logarithm depends linearly on the predictor) between the values in SHAM at both 405 nm and 488 nm. The relationship between the number of nuclei in UUO and SHAM at 488 nm allows us to predict UUO values with respect to SHAM values.

We acknowledge that several factors could have influenced the total number of visible nuclei, such as variability in the contact surface area between the kidney and the coverslip, which corresponds to the examined area and the relatively shallow depth accessible *via* confocal imaging.

Based on these findings, we confirm the results of previous *in vitro* study [16] and recommend the use of 405 nm laser excitation (or close to it, depending on the specific setup of each confocal system) for the *in vivo* quantification of fluorescence intensity. If the goal is represented by nuclear counting, our statistical data recommend the use of 488 nm excitation.

The results of this first study are pointing to an increased oxidative stress in the setting of experimental UUO. A recent Cochrane meta-analysis suggested that CKD patients not receiving dialysis could benefit from antioxidant therapy to prevent further progression towards the end-stage renal disease [31]. Whether initiation of the antioxidant therapy should be done prior or after the constitution of morphological changes remains to be elucidated.

The following study limitations should be mentioned: firstly, we did not perform a longer follow-up in order to assess the status of the oxidative stress at later stages. Second, by using confocal microscopy we were able to visualize only subcortical tubules. Also, we cannot exclude an augmentation of the endogenous antioxidant defense mechanisms in response to the increased OS. Moreover, we did not assess the contribution of other ROS species to the UUO-induced oxidative stress.

Conclusions

We have developed a working model for the dynamic *in vivo* quantification of ROS generation using DHE labeling. We report a significant increase in ROS production in rats subjected to ureteral ligation on the 10th day post-surgery. Our findings suggest that the surgery-related oxidative stress declines after an initial increase in the first days, whereas the one elicited by the chronic ligation continues to increase.

Conflict of interests

The authors declare that they have no conflict of interests.

Acknowledgments

This research did not receive any specific grant from funding agencies in the public, commercial, or not-for-profit sectors.

References

[1] Poyton RO, Ball K, Castello PR. Mitochondrial generation of free radicals and hypoxic signaling. Trends Endocrinol Metab, 2009, 20(7):332–340.
[2] Wang X, Fang H, Huang Z, Shang W, Hou T, Cheng A, Cheng H. Imaging ROS signaling in cells and animals. J Mol Med (Berl), 2013, 91(8):917–927.
[3] Betteridge DJ. What is oxidative stress? Metabolism, 2000, 49(2 Suppl 1):3–8.
[4] Small DM, Coombes JS, Bennett N, Johnson DW, Gobe GC. Oxidative stress, anti-oxidant therapies and chronic kidney disease. Nephrology (Carlton), 2012, 17(4):311–321.
[5] Djamali A, Reese S, Yracheta J, Oberley T, Hullett D, Becker B. Epithelial-to-mesenchymal transition and oxidative stress in chronic allograft nephropathy. Am J Transplant, 2005, 5(3): 500–509.
[6] Djamali A. Oxidative stress as a common pathway to chronic tubulointerstitial injury in kidney allografts. Am J Physiol Renal Physiol, 2007, 293(2):F445–F455.
[7] Dounousi E, Papavasiliou E, Makedou A, Ioannou K, Katopodis KP, Tselepis A, Siamopoulos KC, Tsakiris D. Oxidative stress is progressively enhanced with advancing stages of CKD. Am J Kidney Dis, 2006, 48(5):752–760.
[8] Kim J, Jung KJ, Park KM. Reactive oxygen species differently regulate renal tubular epithelial and interstitial cell proliferation after ischemia and reperfusion injury. Am J Physiol Renal Physiol, 2010, 298(5):F1118–F1129.
[9] Taft DR. The isolated perfused rat kidney model: a useful tool for drug discovery and development. Curr Drug Discov Technol, 2004, 1(1):97–111.
[10] Georgiev T, Iliev R, Mihailova S, Hadzhibozheva P, Ilieva G, Kamburova M, Tolekova A. The isolated perfused kidney models – certain aspects. Trakia J Sci, 2011, 9(3):82–87.
[11] Chang HH, Choong B, Phillips A, Loomes KM. The isolated perfused rat kidney: a technical update. Exp Anim, 2013, 62(1):19–23.
[12] Crawford C, Kennedy-Lydon T, Sprott C, Desai T, Sawbridge L, Munday J, Unwin RJ, Wildman SSP, Peppiatt-Wildman CM. An intact kidney slice model to investigate *vasa recta* properties and function *in situ*. Nephron Physiol, 2012, 120(3):17–31.
[13] Konstantinou D, Mavrakis A, Grintzalis K, Papapostolou I, Assimakopoulos SF, Chroni E, Georgiou C. Quantification of superoxide radical in the brain of rats with experimentally induced obstructive jaundice. Neurochem Res, 2008, 33(6): 1101–1105.
[14] Forkink M, Willems PHGM, Koopman WJH, Grefte S. Live-cell assessment of mitochondrial reactive oxygen species using dihydroethidine. Methods Mol Biol, 2015, 1264:161–169.
[15] Zielonka J, Kalyanaraman B. Hydroethidine- and MitoSOX-derived red fluorescence is not a reliable indicator of intracellular superoxide formation: another inconvenient truth. Free Radic Biol Med, 2010, 48(8):983–1001.
[16] Robinson KM, Janes MS, Pehar M, Monette JS, Ross MF, Hagen TM, Murphy MP, Beckman JS. Selective fluorescent imaging of superoxide *in vivo* using ethidium-based probes. Proc Natl Acad Sci U S A, 2006, 103(41):15038–15043.
[17] Zhan M, Brooks C, Liu F, Sun L, Dong Z. Mitochondrial dynamics: regulatory mechanisms and emerging role in renal pathophysiology. Kidney Int, 2013, 83(4):568–581.
[18] Hernansanz-Agustín P, Izquierdo-Álvarez A, Sánchez-Gómez FJ, Ramos E, Villa-Piña T, Lamas S, Bogdanova A, Martínez-Ruiz A. Acute hypoxia produces a superoxide burst in cells. Free Radic Biol Med, 2014, 71:146–156.
[19] Bräsen JH, Nieminen-Kelhä M, Markmann D, Malle E, Schneider W, Neumayer HH, Budde K, Luft FC, Dragun D. Lectin-like oxidized low-density lipoprotein (LDL) receptor

(LOX-1)-mediated pathway and vascular oxidative injury in older-age rat renal transplants. Kidney Int, 2005, 67(4):1583–1594.
[20] Chevalier RL, Forbes MS, Thornhill BA. Ureteral obstruction as a model of renal interstitial fibrosis and obstructive nephropathy. Kidney Int, 2009, 75(11):1145–1152.
[21] Dunn KW, Sandoval RM, Kelly KJ, Dagher PC, Tanner GA, Atkinson SJ, Bacallao RL, Molitoris BA. Functional studies of the kidney of living animals using multicolor two-photon microscopy. Am J Physiol Cell Physiol, 2002, 283(3):C905–C916.
[22] de Chaumont F, Dallongeville S, Chenouard N, Hervé N, Pop S, Provoost T, Meas-Yedid V, Pankajakshan P, Lecomte T, Le Montagner Y, Lagache T, Dufour A, Olivo-Marin JC. Icy: an open bioimage informatics platform for extended reproducible research. Nat Methods, 2012, 9(7):690–696.
[23] Delgado-Gonzalo R, Uhlmann V, Schmitter D, Unser M. Snakes on a plane: a perfect snap for bioimage analysis. IEEE Signal Process Mag, 2015, 32(1):41–48.
[24] Negrea R. Modelare statistică şi stocastică. Aplicaţii în inginerie şi economie. Ed. Politehnica, Timişoara, 2006.
[25] Agresti A. An introduction to categorical data analysis. Wiley Series in Probability and Statistics, 2nd edition, Wiley–Intersciences, 2007, 204–232.
[26] Okamura DM, Pennathur S. The balance of powers: redox regulation of fibrogenic pathways in kidney injury. Redox Biol, 2015, 6:495–504.
[27] Levonen AL, Hill BG, Kansanen E, Zhang J, Darley-Usmar VM. Redox regulation of antioxidants, autophagy, and the response to stress: implications for electrophile therapeutics. Free Radic Biol Med, 2014, 71:196–207.
[28] Ma J, Nishimura H, Fogo A, Kon V, Inagami T, Ichikawa I. Accelerated fibrosis and collagen deposition develop in the renal interstitium of angiotensin type 2 receptor null mutant mice during ureteral obstruction. Kidney Int, 1998, 53(4): 937–944.
[29] Devi S, Li A, Westhorpe CLV, Lo CY, Abeynaike LD, Snelgrove SL, Hall P, Ooi JD, Sobey CG, Kitching AR, Hickey MJ. Multiphoton imaging reveals a new leukocyte recruitment paradigm in the glomerulus. Nat Med, 2013, 19(1):107–112.
[30] Fernandes DC, Wosniak J Jr, Pescatore LA, Bertoline MA, Liberman M, Laurindo FRM, Santos CXC. Analysis of DHE-derived oxidation products by HPLC in the assessment of superoxide production and NADPH oxidase activity in vascular systems. Am J Physiol Cell Physiol, 2007, 292(1):C413–C422.
[31] Jun M, Venkataraman V, Razavian M, Cooper B, Zoungas S, Ninomiya T, Webster AC, Perkovic V. Antioxidants for chronic kidney disease. Cochrane Database Syst Rev, 2012, 10: CD008176.

Corresponding author
Mirela Danina Muntean, Professor, MD, PhD, Department of Functional Sciences – Pathophysiology, "Victor Babeş" University of Medicine and Pharmacy, 2 Eftimie Murgu Square, 300041 Timişoara, Romania; Phone/Fax +40256–493 085, e-mail: daninamuntean@umft.ro

Received: September 30, 2016

Accepted: December 12, 2017